Transcriptome profiling in the marine red alga *Neopyropia yezoensis* under light/dark cycle

Sayaka Kominami [1], Hiroyuki Mizuta[1], Toshiki Uji[1]

[1] Laboratory of Aquaculture Genetics and Genomics, Division of Marine Life Science, Faculty of Fisheries Sciences, Hokkaido University, Hakodate 041-8611, Japan

***Correspondence**:
Toshiki Uji
E-mail: t-uji@fish.hokudai.ac.jp

Abstract

Many organisms are subjected to a daily cycle of light and darkness, which significantly influences metabolic and physiological processes. In the present study, *Neopyropia yezoensis,* one of the major cultivated seaweeds used in "nori," was harvested in the morning and evening during light/dark treatments to investigate daily changes in gene expression using RNA-sequencing. A high abundance of transcripts in the morning includes the genes associated with carbon–nitrogen assimilations, polyunsaturated fatty acid, and starch synthesis. In contrast, the upregulation of a subset of the genes associated with the pentose phosphate pathway, cell cycle, and DNA replication at evening is necessary for the tight control of light-sensitive processes, such as DNA replication. Additionally, a high abundance of transcripts at dusk encoding asparaginase and glutamate dehydrogenase imply that regulation of asparagine catabolism and tricarboxylic acid cycle possibly contributes to supply nitrogen and carbon, respectively, for growth during the dark. In addition, genes encoding cryptochrome/photolyase family and histone modification proteins were identified as potential key players for regulating diurnal rhythmic genes.

Keywords: *Neopyropia*, red algae, diurnal rhythm, light/dark cycle, RNA-seq

Introduction

Due to the earth's rotation, many organisms encounter changing conditions in their daily environment, such as light and dark. Consequently, the organisms have evolved mechanisms to determine the time of the day and anticipate light/dark shifts in the environment to schedule specific tasks during the day or night (Barinaga 1998). The day/night cycle, also known as diurnal rhythm, is accomplished via systems: light and a free-running internal circadian clock—approximately 24-hour time (Dunlap 1999). Clock genes regulate the timing of various physiological responses, such as growth, development, photosynthesis, and nutrient availability throughout the day by coordinating the expression of numerous output genes (Schaffer et al. 2001; Harmer et al. 2000). The circadian clock is also essential to determine the length of the day or photoperiod for controlling many developmental processes—a well-known phenomenon for regulating flowering time in plants (Imaizumi 2010; Johansson and Staiger 2015).

Since the circadian clock coordinates many aspects of plant growth, metabolism and physiology that contribute to plant performance, circadian clock is an attractive target during breeding for crop improvement (Dodd et al. 2005; McClung 2021). In fact, early farmers and latterly breeders have indirectly selected variation at circadian loci by selecting the highest-yielding varieties in their local environment (Steed et al. 2021). In addition, manipulating circadian oscillator genes could contribute to lead heterosis and hybrid vigor, which refers to the superior performance of the first-generation progeny of crosses compared to their inbred parents (Fujimoto et al. 2018).

Macroalgae display diurnal and circadian rhythms as a part of their physiological processes. For example, all three major macroalgal groups exhibit diurnal and circadian

rhythm in photosynthesis—green algae *Bryopsis maxima* (Okada et al. 1978) and *Ulva compressa* (Kuwano et al. 2008); red algae *Kappaphycus alvarezii* (Granbom et al. 2001; Schubert et al. 2004) and *Grateloupia turuturu* (Goulard et al. 2004); and brown algae *Ectocarpus* sp. (Schmid and Dring 1992) and *Spatoglossum pacificum* (Kageyama et al. 1979). Likewise diurnal and circadian periodicity of mitosis, growth, and spore discharge can be seen in macroalgal groups including the green algae *Ulva pseudocurvat*a (Titlyanov et al. 1996); red algae tropical Florideophyceae (Ngan and Price 1983) and *Porphyra umbilicalis* (Lüning et al. 1997); and brown algae *Nereocystis luetkeana* and *Laminaria* sp. (Amsler and Neushul 1989, Lüning 1994, and Makarov et al. 1995). In terms of photoperiod regulation, in macroalgae's, gametogenesis and sporogenesis are triggered by changes in day length (Breeman 1993, Pang and Lüning 2004, and Choi et al. 2005). Despite the growing body of information on the diurnal and circadian rhythms in the physiological processes of macroalgae, the global expression profiles of diurnal genes and critical molecular players underlying the rhythms remain poorly characterized.

Neopyropia yezoensis (formerly *Pyropia yezoensis*) is a major cultivated macroalga commonly used to wrap sushi and onigiri in the cuisine "nori." Due to its economic importance, several reports on diurnal rhythms in the biological process responsible for growth, such as cell division, photosynthesis and nitrogen uptake have been documented (Oohusa et al. 1997a, b; 1980). Moreover, the amount of total free amino acids increased during light culture and peaked at the end of light period, and then gradually decreased during night in *N. yezoensis* (Oohusa et al. 1997b). The amount and the composition of free amino acids determine the protein quality of food and the taste; for example, alanine has a sweet taste and glutamate elicits umami taste by stimulating

78 the umami receptor (Mouritsen et al. 2019). In terms of reproduction, the formation of
79 conchosporangia in *Neopyropia* species that discharges spores as "nori" seeds are
80 strongly affected by photoperiod (Dring 1967), like the photoperiodic responses of
81 flowering plants. Thus, transcriptome analysis of diurnal rhythms provides the
82 foundation for understanding the molecular mechanisms underlying the growth,
83 reproduction, and metabolism that may be involved in productivity and quality of nori.
84 The present study identified the diurnal regulation of genes associated with
85 physiological processes, such as photosynthesis, nitrogen and amino acids metabolism,
86 and cell division. We further characterized the candidate genes responsible for
87 macroalgae's diurnal and circadian rhythms, which will aid our understanding of their
88 molecular clock mechanism.
89

90 **Materials and methods**

91 **Algal materials**

92 The leafy gametophytes of *N. yezoensis* strain TU-1 were cultured in a medium of
93 sterile vitamin-free Provasoli enriched seawater (Provasoli, 1968) at 15°C under a
94 photoperiod regime of 10 h:14 h light/dark cycle using cool-white fluorescent lamps at
95 40 μmol photons $m^{-2}s^{-1}$ as described in the previous study (Uji et al. 2020). The
96 vegetative gametophytes (ca. 20-mm blade length) were cultured in 500 mL media and
97 harvested at Zeitgeber Time (ZT) 1, 5, 9, 13, 17, 21, and 25 with two biological repeats.
98 The harvested culture was immediately frozen in liquid nitrogen and stored at −80 °C
99 until RNA extraction.

100 **RNA preparation and sequencing**

Total RNA from thalli was extracted in liquid nitrogen with a mortar and pestle using the RNeasy Plant Mini Kit (Qiagen, Hilden, Germany) according to the manufacturer's instructions. The extracted RNA was purified using the TURBO DNA-free kit (Invitrogen/Life Technologies, Carlsbad, CA) to obtain DNA-free RNA. The quantity and integrity of RNA samples were assessed using Nanodrop 2000 Spectrophotometer (Thermo Fisher Scientific, Waltham, MA, USA) and Agilent 2100 Bioanalyzer (Agilent Technologies, Santa Clara, CA, USA). A total of four libraries of complementary DNA (cDNA)—2 conditions: ZT1, ZT9 (×2 replicates each)—were constructed and subsequently sequenced using Illumina Novaseq 6000 instrument at Veritas Genetics.

Assessment of differential gene expression

The RNA-seq analysis was performed using the Galaxy pipeline (Goecks et al. 2010). The FastQC (Wingett and Andrews 2018) toolkit and Trimmomatic (Bolger et al. 2014) were used to assess raw fastq data and to remove the adapter, respectively. Trimmomatic use the following parameters: LEADING: 3, TRAILING: 3, SLIDINGWINDOW: 4: 15, MINLEN: 50. The high-quality reads obtained were mapped to *N. yezoensis* reference genome (Nakamura et al. 2013) using Bowtie2 (Langmead and Salzberg 2012). StringTie (Pertea et al. 2016) was used to create assembly based on the mapping files and then calculated transcripts per kilobase million. Differentially expressed genes (DEGs) between ZT1 and ZT9 (two replicates for each condition) were identified using featureCounts (Liao et al. 2014) and DESeq2 (Love et al. 2014) with a filtering *P*-value of ≤ 0.05 and $|\log_2$ fold change$| > 1$. Afterwards, gene ontology (GO) analysis of specific groups of DEGs was performed using Blast2GO

123 software (Conesa et al. 2005) with the biological process, molecular function and
124 cellular component GO lists.

125 **Quantitative PCR**

126 Quantitative PCR (qPCR) analysis was performed as described by Uji et al. (2019) with
127 minor modification. First-strand cDNA was synthesized from 0.5 μg of total RNA
128 (same RNA used for RNA-seq) using the PrimeScript II 1st strand cDNA Synthesis Kit
129 (TaKaRa Bio, Shiga, Japan). The cDNA was diluted 10-fold for qPCR analysis, and 1.0
130 μl of the diluted cDNA was used as a template in a 20 μL reaction volume using KOD
131 SYBR® qPCR Mix (TOYOBO, Osaka, Japan) following the manufacturer's
132 instructions. Real-time PCR was then performed with a LightCycler® 480 System
133 (Roche Diagnostics, Basel, Switzerland) under the following conditions: 2 min at 98°C
134 followed by 40 cycles of 10 s at 98°C, 10 s at 55°C and 30 s at 68°C. The mRNA levels
135 were calculated using the $2^{-\triangle\triangle Ct}$ method and normalized to levels of 18S ribosomal
136 RNA (*Ny18SrRNA*) gene (Uji et al. 2016). The relative expression level was calculated
137 as a ratio of the mRNA level to the transcription level at ZT1. All the experiments were
138 performed in triplicate. Table S1 lists the primers that were used in this study.
139

140 **Results and discussion**

141 **Identification of DEGs**

142 To begin, we used RNA-seq to compare transcripts in thalli of *N. yezoensis* in the
143 morning and evening to identify genes with diurnal expression. We harvested thalli at 1
144 hour after the onset of light (ZT1, morning) and 1 hour before dark (ZT9, evening)

145 under 10:14 light/dark cycles. In total, ~98.5 million reads were obtained from the deep
146 sequencing with 24.6 million reads per library for four samples (ZT1, ZT9 ×2 replicates
147 each). The number of mapped reads generated from the four libraries were 27.5 (58.1%)
148 and 22.9 (53.8%) million reads, respectively (Table 1).

149 We identified 2,143 DEGs by comparing morning and evening transcripts,
150 indicating that 20.75% of transcripts in *N. yezoensis* display rhythmic expression
151 patterns under the light/dark cycle. Among 2,143 DEGs, we identified the gene
152 encoding sodium transporter (*NyNhaD*) (Fold change: 9.70) that was reported as a
153 diurnal regulated gene in a previous study (Uji et al. 2012). Additionally, qPCR analysis
154 was performed to validate RNA-seq data to reveal detailed expression patterns of genes
155 preferentially expressed in the morning and evening. Twelve DEGs (six each for
156 morning and evening-phased genes) were selected for qPCR analysis to validate
157 RNA-seq data (Table S2). As shown in Fig. 1, the tested genes exhibited a similar level
158 of expression profile in RNA-seq and qPCR analysis, showing that the expression
159 dataset obtained via RNA-seq was valid for the expression pattern of diurnal regulated
160 genes. In the present study, 1,027 and 1,116 genes were identified as preferentially
161 morning and evening-phased genes, respectively.

162 To elucidate the potential biological and molecular functions of these DEGs, we
163 performed GO analysis using the Blast2GO software (Fig. 2). Preferentially
164 morning-phased genes were categorized into the GO term “carbohydrate metabolic
165 process”, “lipid metabolic process”, and “DNA-binding transcription factor activity”. Of
166 the 145 genes from *N. yezoensis* assigned to GO term “carbohydrate metabolic process”,
167 27 genes were morning genes (19% of the annotated the GO term). In GO terms “lipid
168 metabolic process” and “DNA-binding transcription factor activity”, morning genes

accounted for 28% and 46% of total genes to annotated each GO term, respectively. In contrast, preferentially evening-phased genes were characterized “cell cycle” (36%), “DNA replication origin binding” (100%), “DNA replication initiation” (89%), and “chromosome” (28%).

Photosynthesis

The DEGs analysis revealed that a high abundance of transcripts in the morning includes the genes associated with photosynthesis (Table 2). As shown in Fig. 3A, the Calvin–Benson–Bassham cycle (CBB)—the photosynthetic pathway responsible for carbon assimilation—is operated by 11 enzymes that catalyze 13 biological reactions (Sun et al. 2003). In RNA-seq analysis, we found 10 DEG encoding enzymes of the CBB except for the Rubisco gene encoded by the plastid genomes (Table 2, Fig 3A). We used qPCR to assess the expression level of genes encoding the large subunits of Rubisco and other nuclear encoding genes of CBB enzymes because our RNA-seq data did not include transcripts of plastid encoding genes. As shown in Fig. 3B, the transcripts of Calvin cycle genes peaked in the morning, decreased at night, and then gradually increased to dawn. The diurnal variation of photosynthetic capacity in *N. yezoensis* reported in the previous study (Oohusa 1980) is regulated partly at the transcription level according to the present study’s diel rhythms of orchestrated transcription of Calvin cycle genes.

Furthermore, we identified diurnal changes in the *NySIG* gene that encodes nuclear-encoded sigma factor (SIG) homolog (Table 2). SIG regulates transcription of plastid-encoded genes encoding photosynthesis proteins in higher plants by conferring

promoter specificity to plastid-encoded plastid RNA polymerase (Kanamaru and Tanaka 2004; Chi et al. 2015). Thus, the study of *NySIG* is critical for understanding the regulatory mechanisms underlying the expression profiles of chloroplast genes such as *NyrbcL* in daily light-dark cycles.

Calvin cycle provides intermediates required for starch biosynthesis (Zeeman et al. 2010; Geigenberger 2011). In starch biosynthesis of land plants, the first committed step involves the conversion of glucose 1-phosphate (Glc-1-P) and ATP to ADP-Glc and inorganic pyrophosphate (PPi), catalyzed by ADP-Glc pyrophosphorylase (AGPase) (Zeeman et al. 2010; Geigenberger 2011; Qu et al. 2018). ADP-Glc acts as the glucosyl donor for different classes of starch synthases (SS), which lengthen the α-1,4-linked glucan chains of the two insoluble starch polymers amylose and amylopectin. Then, branch points are introduced by starch-branching enzymes (SBE). Red algae accumulate starch granules, known as floridean starch, similar in structure to land plant starches (Meeuse et al. 1960; Yu et al. 2002). Previous studies have suggested that the starch synthesis in red algae proceeds via a UDP glucose-selective α-glucan synthase instead of ADP glucose (Viola et al. 2001). Consistent with the hypothesis, RNA-seq showed that transcripts of the genes encoding UDP-glucose pyrophosphorylase as well as SS and SBE were highly expressed in thalli harvested in the morning (Table 2). The starch synthesized via photosynthesis during the day is important to provide a steady supply of carbon throughout the night.

In *N. yezoensis*, the abundance of transcripts of genes encoding Heat shock protein 70 (Hsp70) and peptidyl-prolyl cis-trans isomerase (PPIase) that function as protein folding chaperones was observed in the morning (Table 2). In addition to the heat stress response, Hsp70 genes in higher plants exhibit a diurnal expression pattern

under isothermal conditions (Li et al. 2000). Moreover, overexpression of Hsp70 improved photoprotection and enhanced restoration of photosystem II (PSII) function, whereas underexpression of Hsp70 caused an increased light sensitivity of PSII in the unicellular green alga *Chlamydomonas reinhardtii* (Schroda et al. 1999). PPIase guarantees correct folding of the D1 protein and a successful assembly of the oxygen-evolving complex, whereas the absence renders the PSII complexes extremely susceptible to photoinhibition (Fu et al. 2007; Sirpio et al. 2008). Likewise, activation of NyHsp70 and NyPPI under illumination may participate in the assembly and maintenance of photosynthetic complexes in *N. yezoensis*.

Maintenance of the thylakoid membranes is also essential for the proper functioning of the photosynthetic machinery because PSII is embedded in the thylakoid membranes that are constituted by a lipid matrix (Kobayashi et al. 2017). Red algae synthesize 18:2 n-6 and 18:3 n-3 from saturated fatty acid 18:0 by delta-9 and delta-12 fatty acid desaturases, respectively (Sun et al. 2015; Cao et al. 2017). Delta-15 fatty acid desaturase catalyzes the introduction of a double bond into 18:2 n-6, while delta-6 desaturase converts 18:3 n-3 and 18:2 n-6 to 18:4 n-3 and 18:3 n-6, respectively. Delta-5 desaturase introduces double-bonds to the delta-5 position of the n-3 and n-6 polyunsaturated fatty acid chain and elongase is necessary for production of long-chain polyunsaturated fatty acid (PUFA) such as eicosapentaenoic acid (EPA). RNA-seq data revealed that transcripts of genes encoding enzymes associated with PUFA synthase pathway, including fatty acid desaturase and elongase, were accumulated in thalli harvested in the morning (Table 2). The upregulation of genes encoding enzymes associated with PUFA synthesis in the morning suggests that the activation of the PUFA synthase pathway is necessary for the structure and stability of the thylakoid membrane.

240

241 **Nitrogen metabolism**

242 Carbon compounds provide the carbon skeletons for nitrogen assimilation to generate
243 the primary amino donors, glutamate (Glu) and glutamine (Gln), that play a role in the
244 biosynthesis of all nitrogenous compounds, including amino acids, proteins, nucleic
245 acids, and chlorophylls (Foyer et al. 2003; Nunes-Nesi et al. 2010). In photosynthetic
246 eukaryotes, nitrogen assimilation is carried out via two major biological processes:
247 inorganic nitrogen is converted to ammonia and then to organic nitrogen (Sanz-Luque et
248 al. 2015). Firstly, nitrate reductase (NR) catalyzes nitrate reduction to nitrite, which is
249 subsequently transported into the chloroplast, and then nitrite reductase (NiR) catalyzes
250 nitrite reduction to ammonium. Next, ammonium is incorporated and assimilated via
251 Gln synthetase (GS) and Glu synthase (GOGAT) cycle. GS carries out inorganic N
252 incorporation into amino acids by transferring ammonium to Glu to form Gln, and
253 GOGAT catalyzes the reductant-dependent conversion of Gln and 2-oxoglutarate (2OG)
254 to two molecules of Glu. In addition to NR and GS, nitrate transporters (NRTs) at the
255 plasma membrane and the chloroplast envelope membrane are also key players in
256 controlling the efficiency of nitrogen assimilation (Fernandez and Galvan 2008). The
257 diurnal expression pattern of *NyNRT* is consistent with the previous report on the diel
258 variation of nitrate uptake in *N. yezoensis* (Oohusa et al. 1977b). As shown in Fig. 3 and
259 4, qPCR analysis revealed that the orchestration of the diurnal patterns of genes
260 encoding enzymes involved in the Calvin cycle and nitrogen assimilation, suggesting
261 that the interaction between C and N metabolism plays a vital role in the growth and
262 development of *N. yezoensis*.

263 The tricarboxylic acid (TCA) cycle is the primary source of carbon skeletons
264 required for ammonia assimilation, and thus links carbon and nitrogen metabolisms
265 (Lancien et al. 2000; Szal and Podgórska 2012). A previous study showed that
266 glutamate dehydrogenase (GDH) can catabolize Glu to 2OG in the TCA cycle, which
267 plays a significant role in the delivery of carbon skeletons under limited C conditions
268 during dark (Miyashita and Good 2008). As shown in Fig. 4A, the *NyGDH* transcription
269 exhibited an opposite expression pattern with genes encoding enzymes involved in
270 carbon and nitrogen assimilation, implying that the increase of *NyGDH* transcripts from
271 dusk to night is important for funnel the C skeletons of Glu into the TCA cycle for
272 energy production under C-limiting conditions during dark (Fig. 4B). In addition, the
273 ammonium released by the GDH reaction may be available for biosynthesis of
274 nitrogenous compounds such as amino acids in *N. yezoensis* cells.
275 Photosynthetic organisms have N- and/or C-sensory systems that monitor the
276 accumulation of molecules such as 2OG, Gln, Glu and NO_3^- (Coruzzi and Bush 2001;
277 Nunes-Nesi et al. 2010). In *Arabidopsis thaliana*, a previous study showed that
278 glutamate receptor-like 1.1 (AtGLR1.1) gene, which encodes the protein with high
279 sequence similarity to the deduced amino acid sequences of the animal ionotropic
280 glutamate receptors (iGLRs), functions as a C/N regulator, and/or sensor (Kang and
281 Turano 2003). Immunoblot, isoenzyme, and RT-PCR analyses indicate that AtGLR1.1
282 regulates the accumulation of N-metabolic enzymes such as GS and NR (Kang and
283 Turano 2003). In contrast, qPCR analysis showed that the diurnal rhythms of transcripts
284 of *NyGLR* gene encoding a homolog of glutamate receptor exhibited an opposite diurnal
285 pattern with *NyGS* and *NyNR*, and a similar expression pattern with *NyGDH* (Fig. 4B).
286 The investigation of downstream signaling of *NyGLR* could lead to elucidate the

mechanisms on the balance between carbon and nitrogen metabolites.

Amino acids metabolism

In addition to nitrogen metabolism, transcripts of genes involved in amino acids metabolism exhibited daily fluctuations. Among amino acids, asparagine is an efficient molecule for the storage and transport of nitrogen because it exhibits an N: C ratio of 2:4 (in contrast to 2:5 for glutamine) (Sieciechowicz et al. 1998; Cánovas et al. 2007, Lea et al. 2007). In the case of asparagine metabolism, asparaginase (ASPG) catalyzes the hydrolysis of asparagine to aspartic acid and ammonium, which is subsequently reassimilated for other nitrogen compound biosynthesis (Grant and Bevan 1994; Lea et al. 2007). Previous studies showed that the mitotic index of thalli in *Neopyropia* and *Porphyra* species exhibited maxima and minima during the night and the day, respectively (Oohusa 1980; Lüning et al. 1997). These results imply that high abundance of ASPG transcripts at dusk (Table 3) may contribute to supply nitrogen to the zone of cell division during the dark through asparagine catabolism.

Several studies have shown the functions of proline as antioxidant (Matysik et al. 2002). For example, proline mediates the suppression of thylakoid lipid peroxidation under illumination by decreasing free radical-induced photodamage (Alia et al. 1997). In eukaryotes, Δ1-pyrroline-5-carboxylate synthetase (P5CS) is a bi-functional enzyme with γ-glutamyl kinase (GK) and γ-glutamyl phosphate reductase (GPR) activities and catalyze the rate-limiting reaction in proline biosynthesis (Hu et al. 1992; Kishor et al. 1995). Previous reports showed that mRNA abundance of P5CS was correlated with proline accumulation in land plants. In contrast, the two separate enzymes (GK and

310 GPR), which are homologous to both the moieties of P5CS, exist in prokaryotes
311 (Delauney and Verma 1993). The present study identified the gene encoding GK that
312 catalyzes the first step of synthesizing proline from glutamate as a preferentially
313 morning-phased gene (Table 2) implying that activation of proline synthesis is
314 necessary for protection of thylakoid lipid peroxidation during the day in *N. yezoensis*.
315

316 **Cell cycle and cell division**

317 The expression of genes associated with cell cycle and cell division was
318 upregulated in the evening (Table 3). In the eukaryotic cell cycle, distinct
319 cyclin-dependent kinases (CDKs)/cyclin complexes are activated during different cell
320 cycle stages and promote the completion of specific cellular events including DNA
321 replication, chromosomal segregation, and mitotic exit (Ohi and Gould 1999). During a
322 normal cell cycle, the progression of cells in the G2 phase to the M phase is triggered by
323 the activation of the cyclin B-dependent Cdc2 kinase (Harashima et al. 2013). The
324 expression level of *NyCYCB* encoding cyclin B peaked at 1 h before darkness (ZT9)
325 (Fig. 5) that is about the same time as initiation of mitosis in *Porphyra* thalli (Lüning et
326 al. 1997), implying that NyCYCB triggers mitosis in *N. yezoensis*.
327 Furthermore, we found diurnal changes in the homologs genes encoding CDC20
328 and 3xHMG-box protein (Fig. 5) that play a pivotal role in normal chromosome
329 segregation in higher plants to ensure mitotic progression regulation and mitotic exit
330 (Antosch et al. 2015; Kapanidou et al. 2017). This result supports the hypothesis that the
331 upregulation of the CDC20 and 3xHMG-box protein during sexual reproduction in *N.*
332 *yezoensis* is necessary for the tight control of cell cycle progress and cell proliferation to

ensure production of spermatia and spores (Yanagisawa et al. 2019). A high abundance of transcripts at dusk also includes the genes associated with chromosome structural organization events, such as structural maintenance of chromosomes family proteins and DNA replication such as DNA polymerase, DNA ligase, topoisomerase, DNA helicase, and DNA replication licensing factor (Table 3). The variations in daily expression of genes associated with cell cycle and DNA replication regulate the diurnal rhythm of cell proliferation in *N. yezoensis*, which protects DNA damage by excessive oxidative stress.

Pentose phosphate pathway (PPP)

The PPP that consists of two routes plays an essential role in the synthesizing nucleotides necessary for DNA replication and cell proliferation (Kowalik et al. 2017; Polat et al. 2021). The oxidative route of PPP (ox-PPP) is a nonreversible metabolic pathway where glucose-6-phosphate (G6P) is transformed into 6-phosphoglucono-δ-lactone by glucose-6-phosphate dehydrogenase (G6PD) and, subsequently, to ribulose-5-phosphate by 6-phosphogluconate dehydrogenase (6PGD) with the concomitant production of nicotinamide adenine dinucleotide phosphate. The ribulose-5-phosphate is then converted to ribose-5-phosphate and used for the biosynthesis of nucleotides. Transketolase (TKT) reactions control the nonoxidative part of the PPP. TKT catalyzes the reverse reactions of glyceraldehyde-3-phosphate and fructose-6-phosphate from glycolysis to the nonoxidative PPP to generate additional ribonucleotides. The previous studies showed that cancer cells that require ribose-phosphate necessary for nucleic acid synthesis employ the nonoxidative PPP to

356 generate ribonucleotides de novo to synthesize RNA and DNA (Boros et al. 1997; 1998).
357 Carbon-tracing experiments demonstrated that, in rapidly proliferating cancer cells,
358 approximately 80% of ribonucleotides are derived from the nonoxidative PPP regulated
359 by an isoform of TKT (Boros et al. 1997; 1998). In this study, the mRNA transcripts of
360 the genes encoding enzymes involved in ox-PPP, such as *NyG6PD* and *Ny6PGD,*
361 peaked at 1 h before darkness (ZT9) and the beginning of the dark period (ZT13),
362 respectively (Fig. 6). Furthermore, we found a similar expression pattern of the gene
363 encoding an isoform of TKT (NyTKT2) with *Ny6PGD* (Fig. 6). These findings suggest
364 that PPP activation during the evening has a significant role in cell proliferation that are
365 required the ribose-phosphate for nucleic acid synthesis. In addition, our previous
366 RNA-seq data (Uji et al. 2016) showed overexpression of *NyG6PD*, *Ny6PGD,* and
367 *NyTKT2* genes during sexual reproduction in *N. yezoensis*, implying that PPP plays an
368 important role in the proliferation of sexual cells as well as vegetative cells by providing
369 nucleic acids, because cell division in mature gametophytes accelerates to produce a
370 number of male gametes in particular.

371 TKL is a dual function enzyme acting in the CBB and nonoxidative PPP. The
372 *Arabidopsis* genome contains two isoforms of TKT. The expression pattern of one
373 homolog from *Arabidopsis* exhibited the similar expression patterns with genes
374 encoding CBB enzymes such as sedoheptulose-1,7-bisphosphatase (SBPase) and
375 phoshoribulokinase (PRK) that only function in the CBB, whereas other homolog is
376 oppositely regulated relative to these genes, suggesting that it has lost the role as a CBB
377 enzyme (Coate and Doyle 2011). In contrast, both isoforms are positively co-regulated
378 with a complete set of ox-PPP such as G6PD and 6PGD, suggesting that they function
379 as enzymes in PPP (Coate and Doyle 2011). As described above, we found two isoforms

of TKT (NyTKT1 and NyTKT2) exhibit the diurnal expression patterns in *N. yezoensis* (Fig. 3 and 6). NyTKT1 that showed a similar expression pattern with CBB enzymes (Fig. 3B) exhibited an opposite diurnal pattern with NyG6PD and Ny6PGD, suggesting TKTs from *N. yezoensis* have completely separate roles in CBB and PPP unlike higher plants.

Extracellular matrix (ECM)

The ECM proteins regulate various signal transduction events by binding to multiple interacting partners, such as other ECM proteins and signal receptors (Kim et al. 2011). In animal cells, integrins are essential cell adhesion receptors that trigger cell proliferation and differentiation by binding to ECM ligands (Takada et al. 2007). *N. yezoensis* appears to be absent in the integrin system, but possesses integrin-related ECM components, such as spondin domain-containing (NySPLs) and fasciclin domain-containing proteins (NyFALs) (Uji et al. 2022). In this study, NySPL4 and novel fasciclin domain-containing proteins (named NyFAL9) were identified as preferentially evening- and morning-phased genes, respectively (Table 2, 3), suggesting that ECM remodeling occurs in daily light-dark cycles. A recent report showed that the expression of *NySPL4* remarkably increased after 1 day of ACC treatment which can induce gametogenesis in *N. yezoensis* (Uji et al. 2022). The finding implicates that high abundance of *NySPL4* transcripts at dusk may involve in cell proliferation during the dark.

Epigenetic modification

The basic packing units of chromatin are nucleosomes, which are octameric complexes

404 of two molecules each of histones H2A, H2B, H3 and H4, around which are wrapped
405 146 bp of DNA. Histones are subjected to an assortment of dynamic and reversible
406 post-translational modifications (e.g. methylation, acetylation, phosphorylation,
407 ubiquitination, etc.) that serve as “histone code” to determine transcriptional activity of
408 marked loci (Jenuwein and Allis 2001). Chromatin remodeling and histone modifying
409 complexes play a central role in most cellular functions and the development of
410 multicellular organisms (Pfluger and Wagner 2007). Among them, MSI1-like WD40
411 repeat (MSIL) proteins are conserved histone-binding proteins in eukaryotes and play a
412 role in hormone signaling, cell proliferation and differentiation by binding histone
413 deacetylases in higher plants and mammals (Hennig et al. 2005). MSIL proteins also
414 function together with Polycomb group histone methyltransferases in mammals, insects
415 and plants (Hennig et al. 2005). In the present study, RNA-seq showed that transcripts
416 of the genes encoding MSIL as well as SET-domain proteins were highly expressed in
417 thalli harvested in the evening (Table 3). SET-domain proteins methylate lysines in
418 histone tails and thereby are essential for the epigenetic maintenance of either repressed
419 or activated transcriptional states (Rea et al. 2000). The variations in daily expression of
420 genes associated with “histone code” suggest histone modifications regulate diurnal
421 transcript level changes, indicating intriguing link the epigenetic modulation and diurnal
422 rhythms in *N. yezoensis*.
423

424 **Cryptochrome/Photolyase family (CPF)**

425 The CPF constitutes a large group of UV-A/blue-light-activated proteins and is
426 functionally divided into two types of proteins: the Photolyases and Cryptochromes

(Oliveri et al. 2014; Fortunato et al. 2015; Mei and Dvornyk 2015). Photolyases are enzymes that utilize light energy to repair UV-induced DNA damages: the cyclobutane pyrimidine dimer or the 6–4 pyrimidine–pyrimidone photoproducts (Sancar 2008). Cryptochromes that are flavin-containing blue light photoreceptors related to photolyases regulate the entrainment of circadian rhythms in both plants and animals (Cashmore 2003; Chaves et al. 2011). For example, cryptochromes from higher plants primarily mediate photoperiodic control of flowering time (Guo et al. 1998; El-Assal et al. 2003). According to their sequence similarities, cryptochromes from a range of organisms can be clustered, more or less, into three subfamilies: plant cryptochromes, animal cryptochromes and cryptochrome-DASH proteins (CRY-DASH) (Lin and Todo 2005). However, the previous studies also suggest that CPFs from diatom and a unicellular green alga have dual functions: DNA repair activity and regulating the circadian clock (Coesel et al. 2009; Heijde et al. 2010). In contrast to higher plants and microalgae, there is little information on the expression pattern and function of CPFs in macroalgae. In *N. yezoensis*, we found five CPFs (NyCPF1-5) that exhibit the variations in daily expression. NyCPF1, 2 have relatively high homology to cryptochrome-DASH that could be transitions between photolyases and cryptochromes (Kiontke et al. 2020), while other NyCPFs are distantly related to any subfamily of cryptochromes. As shown in Fig. 7, the mRNA levels of *NyCPF1* gradually increased during the day, peaked at midnight (ZT17), and then declined. The transcription level of *NyCPF2* reached a maximum at 1 hour before darkness (ZT9) and gradually decreased during the night, which is a similar expression pattern with genes associated with cell cycle and cell division such as *NyCDC20* and *NyCYCB*. In contrast, *NyCPF 3, 4, 5* transcripts peaked at the beginning of the light period (ZT1), gradually decreased during the day, and

reached nadir just before the start of the dark period (ZT9) (Fig. 7), which showed a similar expression pattern with carbon–nitrogen metabolic genes. These results imply that further characterization of the NyCPFs has the potential to unveil the regulatory mechanisms underlying the circadian rhythms that regulate carbon–nitrogen metabolisms and cell cycle in *N. yezoensis*.

Conclusions

The present study revealed diurnal rhythms in transcript abundance of genes associated with photosynthesis, nitrogen and amino acid metabolisms, starch synthesis, PPP, cell cycle, and DNA replication in *N. yezoensis*. In addition, genes encoding CPFs and histone modification proteins were identified as potential key players for regulating diurnal rhythmic genes. Further investigations of molecular mechanisms regulating diurnal rhythm could offer opportunities to improve productivity and quality of nori through breeding of attractive traits for enhancement of the performance such as photosynthesis efficiency, nutrient availability and cell proliferation.

Author statement

TU was responsible for the design of the experiments and interpretation of the data. SK and TU performed the experiments. SK, TU and HM wrote the manuscript. All authors have read and approved the final version of the manuscript.

Acknowledgments

We wish to thank Drs. Katsutoshi Arai and Takafumi Fujimoto (Hokkaido University, Japan) for kindly providing the LightCycler 480 system.

Conflict of interest

The authors declare that this research was conducted in the absence of any commercial or financial relationships that could be construed as a potential conflict of interest.

Data availability statement

The data that support the findings of this study are available from the corresponding author upon reasonable request.

Funding

This work was supported by the Grant-in-Aid for Young Scientists [grant number19K15907 to TU] from the Japan Society for the Promotion of Science.

References

Alia, Saradhi PP, Mohanty P (1997) Involvement of proline in protecting thylakoid membranes against free radical-induced photodamage. J Photochem Photobiol B Biol 38:253-257

Amsler CD, Neushul M (1989) Diel periodicity of spore release from the kelp *Nereocystis luetkeana* (Mertens) Postels *et* Ruprecht. J Exp Mar Biol Ecol 134:117-127

Antosch M, Schubert V, Holzinger P, Houben A, Grasser KD (2015) Mitotic lifecycle of chromosomal 3xHMG-box proteins and the role of their N-terminal domain in the association with rDNA loci and proteolysis. New Phytol 208:1067–1077

Barinaga M (1998) Circadian rhythms - Clock photoreceptor shared by plants and animals. Science 282:1628-1630

Bolger AM, Lohse M, Usadel B (2014) Trimmomatic: a flexible trimmer for Illumina sequence data. Bioinformatics 30: 2114–2120

Boros LG, Lee PW, Brandes JL, Cascante M, Muscarella P, Schirmer WJ, Melvin WS, Ellison EC (1998) Nonoxidative pentose phosphate pathways and their direct role in ribose synthesis in tumors: is cancer a disease of cellular glucose metabolism? Med Hypotheses 50:55-59

Boros LG, Puigjaner J, Cascante M, Lee W-NP, Brandes JL, Bassilian S, Yusuf FI, Williams RD, Muscarella P, Melvin WS, Schirmer WJ (1997) Oxythiamine and dehydroepiandrosterone inhibit the nonoxidative synthesis of ribose and tumor cell proliferation. Cancer Res 57: 4242-4248

511 Breeman AM (1993) Photoperiodic history affects the critical daylength of the short
512 day-plant *Acrosymphyton purpuriferum* (Rhodophyta). Eur J Phycol 28:157–
513 160

514 Cánovas FM, Avila C, Cantón FR, Cañas RA, De La Torre F (2007) Ammonium
515 assimilation and amino acid metabolism in conifers. J Exp Bot 58: 2307-2318

516 Cao M, Wang D, Mao Y, Kong F, Bi G, Xing Q, Weng Z (2017) Integrating
517 transcriptomics and metabolomics to characterize the regulation of EPA
518 biosynthesis in response to cold stress in seaweed *Bangia fuscopurpurea*. PLoS
519 One 12:e0186986

520 Cashmore AR (2003) Cryptochromes: Enabling plants and animals to determine
521 circadian time. Cell 114: 537-543

522 Chaves I, Pokorny R, Byrdin M, Hoang N, Ritz T, Brettel K, Essen LO, van der Horst
523 GTJ, Batschauer A, Ahmad M (2011) The cryptochromes: blue light
524 photoreceptors in plants and animals. Annu Rev Plant Biol 62:335-364

525 Chi W, He B, Mao J, Jiang J, Zhang L (2015) Plastid sigma factors: their individual
526 functions and regulation in transcription. Biochim Biophys Acta-Bioenergetics
527 1847:770–778

528 Choi HG, Kim YS, Lee SJ, Park EJ, Nam KW (2005) Effects of daylength, irradiance
529 and settlement density on the growth and reproduction of *Undaria pinnatifida*
530 gametophytes. J Appl Phycol 17: 423-430

531 Coate JE, Doyle JJ. (2011) Divergent evolutionary fates of major photosynthetic gene
532 networks following gene and whole genome duplications. Plant Signal Behav
533 6:594-597

534 Coesel S, Mangogna M, Ishikawa T, Heijde M, Rogato A, Finazzi G, Todo T, Bowler
535 C, Falciatore A (2009) Diatom PtCPF1 is a new cryptochrome/photolyase
536 family member with DNA repair and transcription regulation activity. EMBO
537 Rep 10: 655–661

538 Conesa A, Götz S, García-Gómez JM, Terol J, Talón M, Robles M (2005) Blast2GO: a
539 universal tool for annotation, visualization and analysis in functional genomics
540 research. Bioinformatics 21: 3674–3676

541 Coruzzi G, Bush DR (2001) Nitrogen and carbon nutrient and metabolite signaling in
542 plants. Plant Physiol 125:61-64

543 Delauney AJ, Verma DPS (1993) Proline biosynthesis and osmoregulation in plants.
544 Plant J 4: 215-223

545 Dodd AN, Salathia N, Hall A, Kévei E, Tóth R, Nagy F, Hibberd JM, Millar AJ, Webb
546 AAR (2005) Plant circadian clocks increase photosynthesis, growth, survival,
547 and competitive advantage. Science 309:630–633

548 Dring MJ (1967) Effects of daylength on growth and reproduction of
549 conchocelis-phase of *Porphyra tenera*. J Mar Biol Ass UK 47: 501–510

550 Dunlap JC (1999) Molecular bases for circadian clocks. Cell 96: 271-290

551 El-Assal SED, Alonso-Blanco C, Peeters AJM, Wagemaker C, Weller JL, Koornneef
552 M. (2003) The role of cryptochrome 2 in flowering in *Arabidopsis*. Plant
553 Physiol 133:1504–1516

554 Fernandez E, Galvan A (2008) Nitrate assimilation in *Chlamydomonas*. Eukaryot Cell
555 7:555-559

556 Fortunato AE, Annunziata R, Jaubert M, Bouly JP, Falciatore A (2015) Dealing with
557 light: the widespread and multitasking cryptochrome/photolyase family in
558 photosynthetic organisms. J Plant Physiol 172: 42-54

559 Foyer CH, Parry M, Noctor G (2003) Markers and signals associated with nitrogen
560 assimilation in higher plants. J Exp Bot 54: 585-593

561 Fu A, He ZY, Cho HS, Lima A, Buchanan BB, Luan S (2007) A chloroplast
562 cyclophilin functions in the assembly and maintenance of photosystem II in
563 *Arabidopsis thaliana*. Proc Natl Acad Sci USA 104: 15947-15952

564 Fujimoto R, Uezono K, Ishikura S, Osabe K, Peacock WJ, Dennis ES (2018) Recent
565 research on the mechanism of heterosis is important for crop and vegetable
566 breeding systems. Breed Sci 68: 145–158

567 Geigenberger P (2011) Regulation of starch biosynthesis in response to a fluctuating
568 environment. Plant Physiol 155: 1566-1577

569 Goecks J, Nekrutenko A, Taylor J; Galaxy Team. (2010) Galaxy: a comprehensive
570 approach for supporting accessible, reproducible, and transparent computational
571 research in the life sciences. Genome Biol 11:R86

572 Granbom M, Pedersen M, Kadel P, Lüning K (2001) Circadian rhythm of
573 photosynthetic oxygen evolution in *Kappaphycus alvarezii* (Rhodophyta):
574 dependence on light quantity and quality. J Phycol 37: 1020-1025

575 Grant M, Bevan MW (1994) Asparaginase gene expression is regulated in a complex
576 spatial and temporal pattern in nitrogen sink-tissues. Plant J 5: 695-704

577 Guo H, Yang H, Mockler TC, Lin C (1998) Regulations of flowering time by
578 *Arabidopsis* photoreceptors. Science 279:1360–1363

579 Harashima H, Dissmeyer N, Schnittger A (2013) Cell cycle control across the
580 eukaryotic kingdom. Trends Cell Biol 23: 345-356

581 Harmer SL, Hogenesch JB, Straume M, Chang HS, Han B, Zhu T, Wang X, Kreps JA,
582 Kay SA (2000) Orchestrated transcription of key pathways in *Arabidopsis* by
583 the circadian clock. Science 290: 2110-2113

584 Heijde M, Zabulon G, Corellou F, Ishikawa T, Brazard J, Usman A, Sanchez F, Plaza P,
585 Martin M, Falciatore A, Todo T, Bouget FY, Bowler C. (2010) Characterization
586 of two members of the cryptochrome/photolyase family from *Ostreococcus*
587 *tauri* provides insights into the origin and evolution of cryptochromes. Plant
588 Cell Environ 33:1614-1626

589 Hennig L, Bouveret R, Gruissem W (2005) MSI1-like proteins: an escort service for
590 chromatin assembly and remodeling complexes. Trends Cell Biol 15: 295–302

591 Hu CAA, Delauney AJ, Verma DPS (1992) A bifunctional enzyme (delta
592 1-pyrroline-5-carboxylate synthetase) catalyzes the first two steps in proline
593 biosynthesis in plants. Proc Natl Acad Sci USA 89: 9354-9358

594 Imaizumi T (2010) *Arabidopsis* circadian clock and photoperiodism: time to think
595 about location. Curr Opin Plant Biol 13: 83-89

596 Jenuwein T, Allis CD (2001) Translating the histone code. Science 293:1074-1080

597 Johansson M, Staiger D (2015) Time to flower: interplay between photoperiod and the
598 circadian clock. J Exp Bot 66:719-30

599 Kageyama A, Yokohama Y, Nisizawa K (1979) Diurnal rhythm of apparent
600 photosynthesis of a brown alga, *Spatoglossum pacificum*. Bot Mar 22: 199-201

601 Kanamaru K, Tanaka K (2004) Roles of chloroplast RNA polymerase sigma factors in
602 chloroplast development and stress response in higher plants. Biosci Biotechnol
603 Biochem 68:2215–2223
604
605 Kang J, Turano FJ (2003) The putative glutamate receptor 1.1 (AtGLR1.1) functions as
606 a regulator of carbon and nitrogen metabolism in *Arabidopsis thaliana*. Proc Natl
607 Acad Sci USA 100: 6872–6877
608 Kapanidou M, Curtis NL, Bolanos-Garcia VM (2017) Cdc20: At the crossroads
609 between chromosome segregation and mitotic exit. Trends Biochem Sci 42: 193–
610 205
611 Kim SH, Turnbull J, Guimond S (2011) Extracellular matrix and cell signalling: the
612 dynamic cooperation of integrin, proteoglycan and growth factor receptor. J
613 Endocrinol 209: 139–151
614 Kiontke S, Göbel T, Brych A, Batschauer A (2020) DASH-type cryptochromes-solved
615 and open questions. Biol Chem 401:1487-1493

616 Kishor P, Hong Z, Miao GH, Hu C, Verma D (1995) Overexpression of
617 [delta]-pyrroline-5-carboxylate synthetase increases proline production and
618 confers osmotolerance in transgenic plants. Plant Physiol 108: 1387-1394

619 Kobayashi K, Endo K, Wada H (2017) Specific distribution of phosphatidylglycerol to
620 photosystem complexes in the thylakoid membrane. Front Plant Sci 8:1991

621 Kowalik MA, Columbano A, Perra A (2017) Emerging role of the pentose phosphate
622 pathway in hepatocellular carcinoma. Front Oncol 7:87

623 Kuwano K, Sakurai R, Motozu Y, Kitade Y, Saga N (2008) Diurnal cell division
624 regulated by gating the G1/S transition in *Enteromorpha compressa*
625 (Chlorophyta). J Phycol 44: 364-373

626 Lancien M, Gadal P, Hodges M (2000) Enzyme redundancy and the importance of
627 2-oxoglutarate in higher plant ammonium assimilation. Plant Physiol 123:
628 817-824

629 Langmead B, Salzberg SL (2012) Fast gapped-read alignment with Bowtie 2. Nat
630 Methods 9:357-359

631 Lea PJ, Sodek L, Parry MAJ, Shewry PR, Halford NG (2007) Asparagine in plants.
632 Ann Appl Biol 150: 1-26

633 Li QB, Haskell D, Zhang C, Sung DY, Guy C (2000) Diurnal regulation of Hsp70s in
634 leaf tissue. Plant J 21: 373-378

635 Liao Y, Smyth GK, Shi W. (2014) featureCounts: an efficient general purpose program
636 for assigning sequence reads to genomic features. Bioinformatics. 30:923-30

637 Lin C, Todo, T (2005) The cryptochromes. Genome biol 6: 220

638 Lüning K (1994) Circadian growth rhythm in juvenile sporophytes of Laminariales
639 (Phaeophyta). J Phycol 30: 193-199

640 Lüning K, Titlyanov EA, Titlyanova TV (1997) Diurnal and circadian periodicity of
641 mitosis and growth in marine macroalgae .III. The red alga *Porphyra*
642 *umbilicalis*. Eur J Phycol 32: 167-173

643 Love MI, Huber W, Anders S (2014) Moderated estimation of fold change and
644 dispersion for RNA-seq data with DESeq2. Genome Biol 15:550

645 Makarov VN, Schoschina EV, Luning K (1995) Diurnal and circadian periodicity of
646 mitosis and growth in marine macroalgae .I. Juvenile sporophytes of
647 *Laminariales* (Phaeophyta). Eur J Phycol 30: 261-266

Matysik J, Alia Bhalu B, Mohanty P (2002) Molecular mechanisms of quenching of reactive oxygen species by proline under stress in plants. Curr Sci 82: 525-532

McClung CR (2021) Circadian clock components offer targets for crop domestication and improvement. Genes 12: 374

Meeuse BJD, Andries M, Wood JA (1960) Floridean Starch. J Exp Bot 11: 129

Mei QM, Dvornyk V (2015) Evolutionary history of the photolyase/cryptochrome superfamily in eukaryotes. PLoS One 10:9

Miyashita Y, Good AG (2008) NAD(H)-dependent glutamate dehydrogenase is essential for the survival of *Arabidopsis thaliana* during dark-induced carbon starvation. J Exp Bot 59: 667-680

Mouritsen OG, Duelund L, Petersen MA, Hartmann AL, Frøst MB (2019) Umami taste, free amino acid composition, and volatile compounds of brown seaweeds. J Appl Phycol 31: 1213–1232

Nakamura Y, Sasaki N, Kobayashi M, Ojima N, Yasuike M, Shigenobu Y, Satomi M, Fukuma Y, Shiwaku K, Tsujimoto A, Kobayashi T, Nakayama I, Ito F, Nakajima K, Sano M, Wada T, Kuhara S, Inouye K, Gojobori T, Ikeo K (2013) The first symbiont-free genome sequence of marine red alga, susabi-nori (*Pyropia yezoensis*). PLoS One 8:e57122

Ngan Y, Price IR (1983) Periodicity of spore discharge in tropical Florideophyceae (Rhodophyta). Br Phycol J 18: 83-95

Nunes-Nesi A, Fernie AR, Stitt M (2010) Metabolic and signaling aspects underpinning the regulation of plant carbon nitrogen interactions. Mol Plant 3:973-996

Ohi R, Gould KL (1999) Regulating the onset of mitosis. Curr Opin Cell Biol 11: 267-273

Okada M, Inoue M, Ikeda T (1978) Circadian rhythm in photosynthesis of the green alga *Bryopsis maxima*. Plant Cell Physiol 19: 197–202

675 Oliveri P, Fortunato AE, Petrone L, Ishikawa-Fujiwara T, Kobayashi Y, Todo T,
676 Antonova O, Arboleda E, Zantke J, Tessmar-Raible K, Falciatore A (2014) The
677 Cryptochrome/Photolyase Family in aquatic organisms. Mar Genomics 14:
678 23-37

679 Oohusa T (1980) Diurnal rhythm in the rates of cell division, growth and
680 photosynthesis of *Porphyra yezoensis* (Rhodophyceae) Cultured in the
681 laboratory. Bot Mar 23: 1-5

682 Oohusa T, Araki S, Sakurai T, Saitoh M (1977a). Physiological studies on diurnal
683 biological rhythms of *Porphyra* .I. Cell-size, physiological-activity and content
684 of photosynthetic pigments in thallus cultured in laboratory. Bull Jpn Soc Sci
685 Fish 43: 245-249

686 Oohusa T, Araki S, Sakurai T, Saitoh M (1977b) Physiological studies on diurnal
687 biological rhythms of *Porphyra* .II. Growth and contents of free and total
688 nitrogen and carbohydrate in thallus cultured in laboratory. Bull Jpn Soc Sci
689 Fish 43: 251-254

690 Pang SJ, Lüning K (2004) Photoperiodic long-day control of sporophyll and hair
691 formation in the brown alga *Undaria pinnatifida*. J Appl Phycol 16: 83-92

692 Pertea M, Kim D, Pertea GM, Leek JT, Salzberg SL (2016) Transcript-level expression
693 analysis of RNA-seq experiments with HISAT, StringTie and Ballgown. Nat
694 Protoc 11: 1650-1667

695 Pfluger J, Wagner D (2007) Histone modifications and dynamic regulation of genome
696 accessibility in plants. Curr Opin Plant Biol 10:645-652

697 Polat IH, Tarrado-Castellarnau M, Bharat R, Perarnau J, Benito A, Cortés R, Sabatier P,
698 Cascante M (2021) Oxidative pentose phosphate pathway enzyme
699 6-phosphogluconate dehydrogenase plays a key role in breast cancer
700 metabolism. Biology 10:85

701 Provasoli L (1968) Media and prospects for the cultivation of marine algae. In:
702 Watanabe A, Hattori A (eds) Culture and collections of algae, Proc U S-Japan
703 Conf, Hakone, September 1966. Jpn Soc Plant Physiol Tokyo, 63–75

Qu J, Xu S, Zhang Z, Chen G, Zhong Y, Liu L, Zhang R, Xue J, Guo D (2018) Evolutionary, structural and expression analysis of core genes involved in starch synthesis. Sci Rep 8:12736

Rea S, Eisenhaber F, O'Carroll D, Strahl BD, Sun ZW, Schmid M, Opravil S, Mechtler K, Ponting CP, Allis CD, Jenuwein T (2000) Regulation of chromatin structure by site-specific histone H3 methyltransferases. Nature 406: 593–599

Sancar A (2008) Structure and function of photolyase and *in vivo* enzymology: 50th anniversary. J Biol Chem 283: 32153-32157

Sanz-Luque E, Chamizo-Ampudia A, Llamas A, Galvan A, Fernandez E (2015) Understanding nitrate assimilation and its regulation in microalgae. Front Plant Sci 6:899

Schaffer R, Landgraf J, Accerbi M, Simon V, Larson M, Wisman E (2001) Microarray analysis of diurnal and circadian-regulated genes in *Arabidopsis*. Plant Cell 13: 113-123

Schmid R, Dring MJ (1992) Circadian rhythm and fast responses to blue light of photosynthesis in *Ectocarpus* (Phaeophyta, Ectocarpales) .I. Characterization of the rhythm and the blue light response. Planta 187: 53-59

Schroda M, Vallon O, Wollman FA, Beck CF (1999) A chloroplast-targeted heat shock protein 70 (HSP70) contributes to the photoprotection and repair of photosystem II during and after photoinhibition. Plant Cell 11: 1165-1178

Schubert H, Gerbersdorf S, Titlyanov E, Titlyanova T, Granbom M, Pape C, Lüning K (2004) Circadian rhythm of photosynthesis in *Kappaphycus alvarezii* (Rhodophyta): independence of the cell cycle and possible photosynthetic clock targets. Eur J Phycol 39: 423-430

Sieciechowicz KA, Joy KW, Ireland RJ (1988) The metabolism of asparagine in plants. Phytochemistry 27: 663-671

Sirpio S, Khrouchtchova A, Allahverdiyeva Y, Hansson M, Fristedt R, Vener AV, Scheller HV, Jensen PE, Haldrup A, Aro EM (2008) AtCYP38 ensures early

biogenesis, correct assembly and sustenance of photosystem II. Plant J 55: 639-651

Steed G, Ramirez DC, Hannah MA, Webb AAR (2021) Chronoculture, harnessing the circadian clock to improve crop yield and sustainability. Science 372: eabc9141

Sun N, Ma LG, Pan DY, Zhao HY, Deng XW (2003) Evaluation of light regulatory potential of Calvin cycle steps based on large-scale gene expression profiling data. Plant Mol Biol 53: 467-478

Sun P, Mao Y, Li G, Cao M, Kong F, Wang L, Bi G (2015) Comparative transcriptome profiling of *Pyropia yezoensis* (Ueda) M.S. Hwang & H.G. Choi in response to temperature stresses. BMC Genomics 16:463

Szal B, Podgórska A (2012) The role of mitochondria in leaf nitrogen metabolism. Plant Cell Environ 35:1756-1768

Takada Y, Ye X, Simon S (2007) The integrins. Genome Biol 8: 215

Titlyanov EA, Titlyanova TV, Lüning (1996) Diurnal and circadian periodicity of mitosis and growth in marine macroalgae .II. The green alga *Ulva pseudocurvata*. Eur J Phycol 31: 181-188

Uji T, Endo H, Mizuta H (2020) Sexual reproduction via a 1-aminocyclopropane-1-carboxylic acid-dependent pathway through redox modulation in the marine red alga *Pyropia yezoensis* (Rhodophyta). Front Plant Sci 11:60

Uji T, Matsuda R, Takechi K, Takano H, Mizuta H, Takio S (2016) Ethylene regulation of sexual reproduction in the marine red alga *Pyropia yezoensis* (Rhodophyta). J Appl Phycol 28: 3501–3509

Uji T, Gondaira Y, Fukuda S, Mizuta H, Saga N (2019) Characterization and expression profiles of small heat shock proteins in the marine red alga *Pyropia yezoensis*. Cell Stress Chaperones 24:223–233

Uji T, Monma R, Mizuta H, Saga N (2012) Molecular characterization and expression analysis of two Na^+/H^+ antiporter genes in the marine red alga *Porphyra yezoensis*. Fisheries Sci 78: 985–991

Uji T, Ueda S, Mizuta H (2022) Identification, characterization, and expression analysis of spondin-like and fasciclin-like genes in *Neopyropia yezoensis*, a marine red alga. Phycology 2:45-59

Viola R, Nyvall P, Pedersén M (2001) The unique features of starch metabolism in red algae. Proc Royal Soc B 268: 1417-1422

Wingett SW, Andrews S (2018) FastQ Screen: a tool for multi-genome mapping and quality control. F1000Research 7:1338

Yanagisawa R, Sekine N, Mizuta H, Uji T (2019) Transcriptomic analysis under ethylene precursor treatment uncovers the regulation of gene expression linked to sexual reproduction in the dioecious red alga *Pyropia pseudolinearis*. J Appl Phycol 31: 3317–3329

Yu S, Blennow A, Bojko M, Madsen F, Olsen CE, Engelsen SB (2002) Physico-chemical characterization of floridean starch of red algae. Starch 54: 66–74

Zeeman SC, Kossmann J, Smith AM. (2010) Starch: its metabolism, evolution, and biotechnological modification in plants. Annu Rev Plant Biol 61: 209–234

Figure legends

Fig. 1 Comparison of gene expression data obtained by RNA-seq and quantitative polymerase chain reaction (qPCR). qPCR analysis was performed on 12 selected genes that showed a difference in expression levels between morning and evening in *N. yezoensis* (red boxes). The gene expression levels obtained from RNA-seq data are

784 indicated by blue boxes (RNA-seq). RNA samples were prepared from thalli harvested
785 at Zeitgeber Time 1 (ZT1) and Zeitgeber Time 9 (ZT9). Results are presented as relative
786 expression compared with that in ZT1. Table S2 lists the genes that were used for the
787 validation.
788
789 Fig. 2 Gene Ontology (GO) classifications of expressed functionally annotated DEGs
790 between morning and evening in *N. yezoensis*. The genes corresponded to three main
791 categories, biological process, molecular function and cellular component.
792
793 Fig. 3 Diurnal expression pattern of genes associated with carbon assimilation in *N.*
794 *yezoensis*.
795 (A) Expression levels of genes encoding enzymes of Calvin–Benson–Bassham cycle
796 (CBB) determined by RNA-Seq. Fold changes in RNA-seq data are presented as
797 relative expression compared between ZT1 and ZT9. The enzymes of CBB are
798 indicated in orange ellipses. Asterisks indicate the enzymes are encoded by the plastid
799 genome Enzymes: RUBISCO, ribulose-1,5-bisphosphate carboxylase/oxygenase; PGK,
800 phosphoglyceratekinase; GAPDH, glyceraldehyde-3-phosphate dehydrogenase; TPI,
801 triosephosphate isomerase; FBA, fructose-1,6-bisphosphate aldolase; FBP,
802 fructose-1,6-bisphosphatase; TK, transketolase; SBP, sedoheptulose-1,7-bisphosphatase;
803 RPE, ribulose-5-phosphate3-epimerase; RPI, ribose-5-phosphate isomerase; PRK,
804 phosphoribulokinase. Metabolites: RuBP, ribulose-1,5-bisphosphate; 3-PGA,
805 3-phosphoglycerate; 1,3-PGA, 1,3-bisphosphoglycerate; G3P,
806 glyceraldehyde-3-phosphate; DHAP, dihydroxyacetone phosphate; F1,6P,
807 fructose-1,6-bisphosphate; F6P, fructose-6-phosphate; X5P, xylulose-5-phosphate; E4P,

erythrose-4-phosphate; S1,7P, sedoheptulose-1,7-bisphosphate; S7P, sedoheptulose-7-phosphate; R5P, ribulose-5-phosphate; Ru5P, ribulose-5-phosphate.

(B) Expression levels of genes encoding enzymes of CBB determined by qPCR.

RNA samples were prepared thalli harvested at ZT (Zeitgeber Time) 1, 5, 9, 13, 17, 21, and 25. Results are presented as relative expression compared with that in ZT1. All data are presented as mean ± SD of three independent experiments. rbcL, large subunit of ribulose-1,5-bisphosphate carboxylase/oxygenase.

Fig. 4 Diurnal expression pattern of genes associated with nitrogen metabolism in *N. yezoensis*.

(A) Expression levels of genes encoding enzymes of nitrogen metabolism determined by qPCR. Results are presented as relative expression compared with that in ZT1. All data are presented as mean ± SD of three independent experiments. GS, glutamine synthetase; NRT, nitrate transporter; NR, nitrate reductase; GDH, glutamate dehydrogenase; GLR, glutamate receptor-like.

(B) Predicted nitrogen metabolism during light and dark cycle in *N. yezoensis*.

Red and blue arrows indicate upregulated and downregulated expression, respectively. GOGAT, glutamate synthase.

Fig. 5 Diurnal expression pattern of genes associated with cell cycle and cell division in *N. yezoensis*. Results are presented as relative expression compared with that in ZT1. All data are presented as mean ± SD of three independent experiments. CYCB, cyclin B; CDC20, Cell Division Cycle 20; HMG, high mobility group.

832

833 Fig. 6 Diurnal expression pattern of genes associated with pentose phosphate pathway
834 in *N. yezoensis*. Results are presented as relative expression compared with that in ZT1.
835 Results are presented as relative expression compared with that in ZT1. All data are
836 presented as mean ± SD of three independent experiments. G6PD, glucose-6-phosphate
837 dehydrogenase; 6PGD, 6-phosphogluconate dehydrogenase; TKT2, transketolase 2.

838

839 Fig. 7 Diurnal expression pattern of Cryptochrome/Photolyase Family (CPF) genes in *N.*
840 *yezoensis*. Results are presented as relative expression compared with that in ZT1. All
841 data are presented as mean ± SD of three independent experiments.

842

843

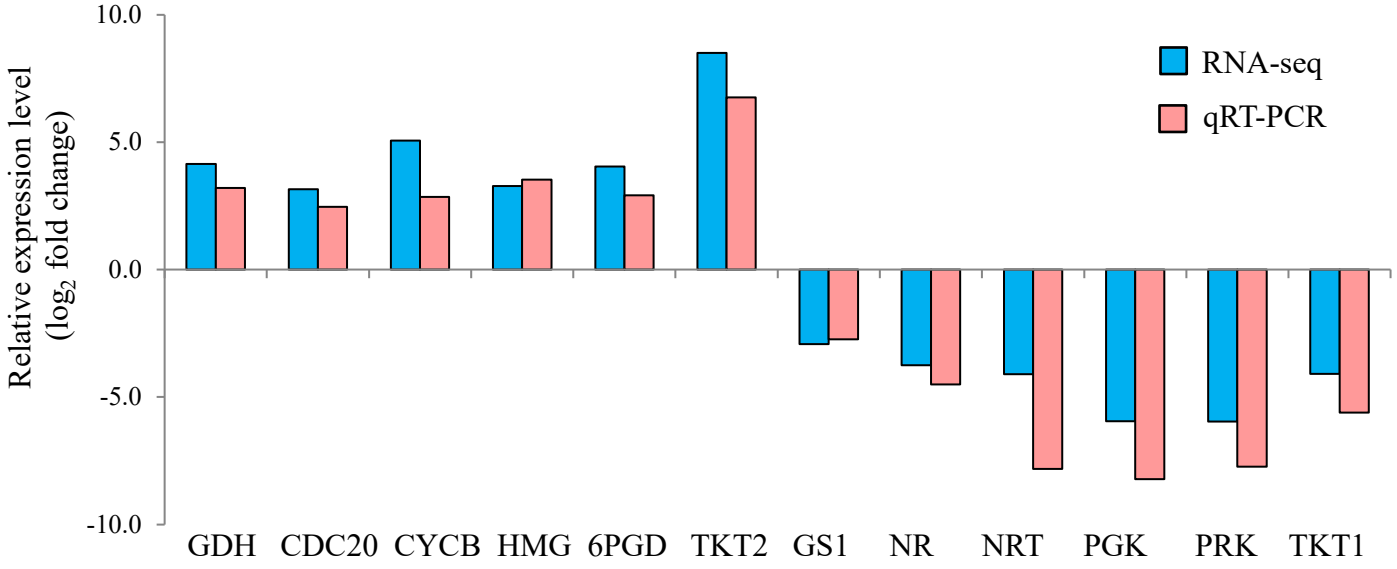
10.0
5.0
0.0
-5.0
-10.0
Relative expression level
(log2 fold change)
RNA-seq
qRT-PCR
GDH
CDC20
CYCB
HMG
6PGD
TKT2
GS1
NR
NRT
PGK
PRK
TKT1

Fig. 1

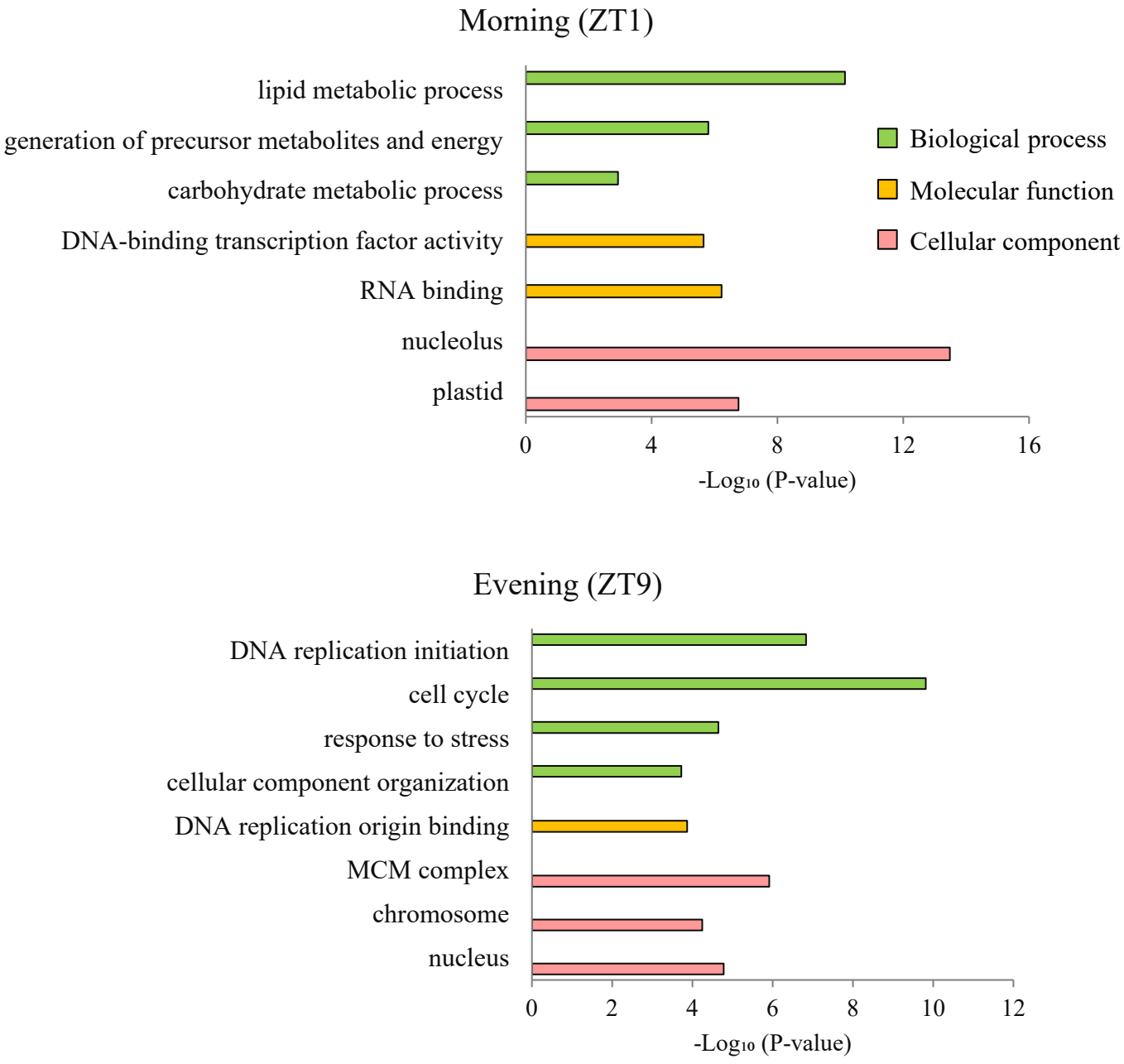
Morning (ZT1)
lipid metabolic process
generation of precursor metabolites and energy
carbohydrate metabolic process
DNA-binding transcription factor activity
RNA binding
nucleolus
plastid
Biological process
Molecular function
Cellular component
0
4
8
12
16
-Log10 (P-value)
Evening (ZT9)
DNA replication initiation
cell cycle
response to stress
cellular component organization
DNA replication origin binding
MCM complex
chromosome
nucleus
0
2
4
6
8
10
12
-Log10 (P-value)

Fig. 2

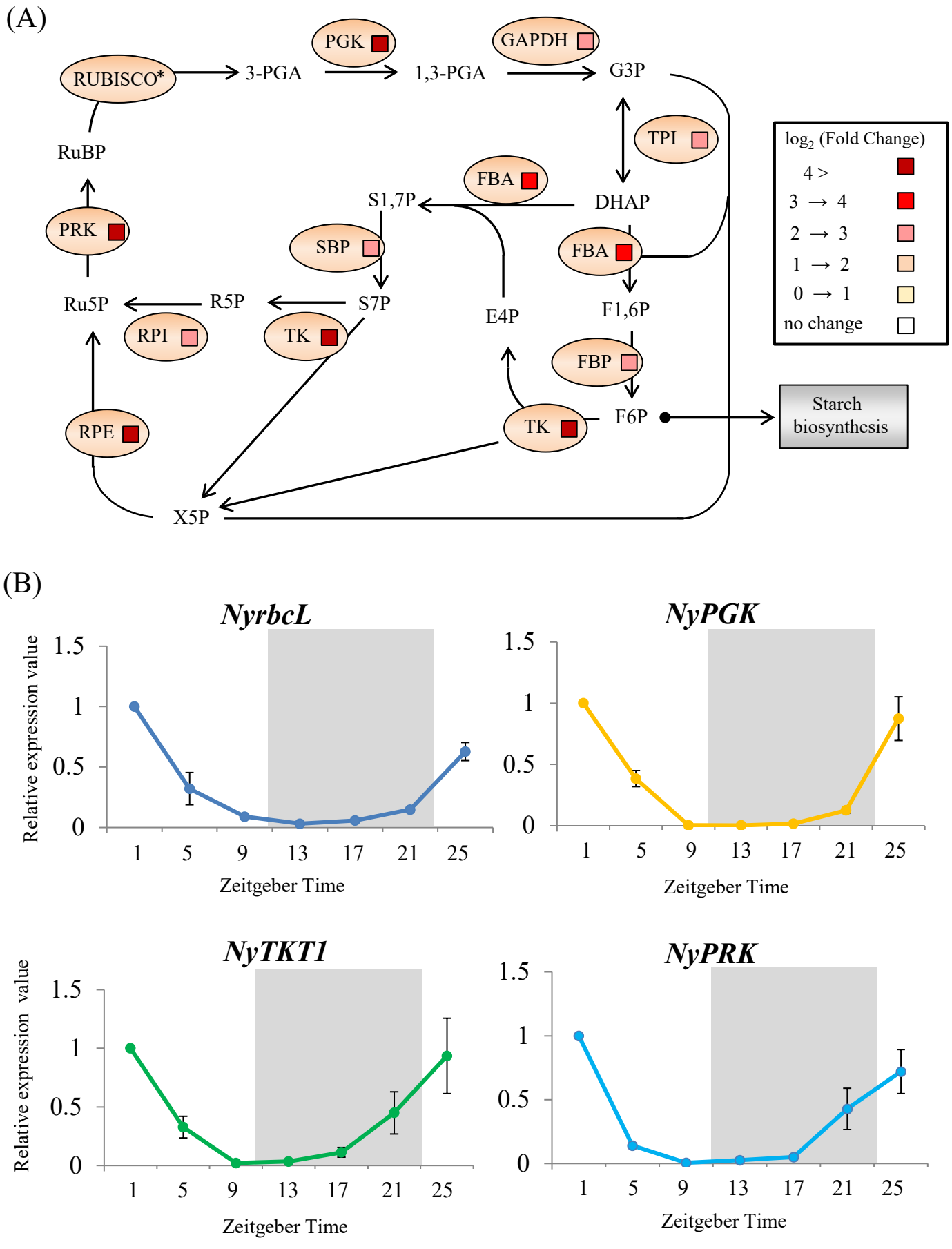
(A)
RUBISCO*
3-PGA
PGK
1,3-PGA
GAPDH
G3P
TPI
DHAP
FBA
S1,7P
SBP
S7P
FBA
F1,6P
E4P
FBP
F6P
TK
TK
RuBP
PRK
Ru5P
R5P
RPI
RPE
X5P
Starch biosynthesis
log2 (Fold Change)
4 >
3 → 4
2 → 3
1 → 2
0 → 1
no change
(B)
NyrbcL
NyPGK
NyTKT1
NyPRK
Relative expression value
Zeitgeber Time
1.5
1
0.5
0
1
5
9
13
17
21
25

Fig. 3

(A)

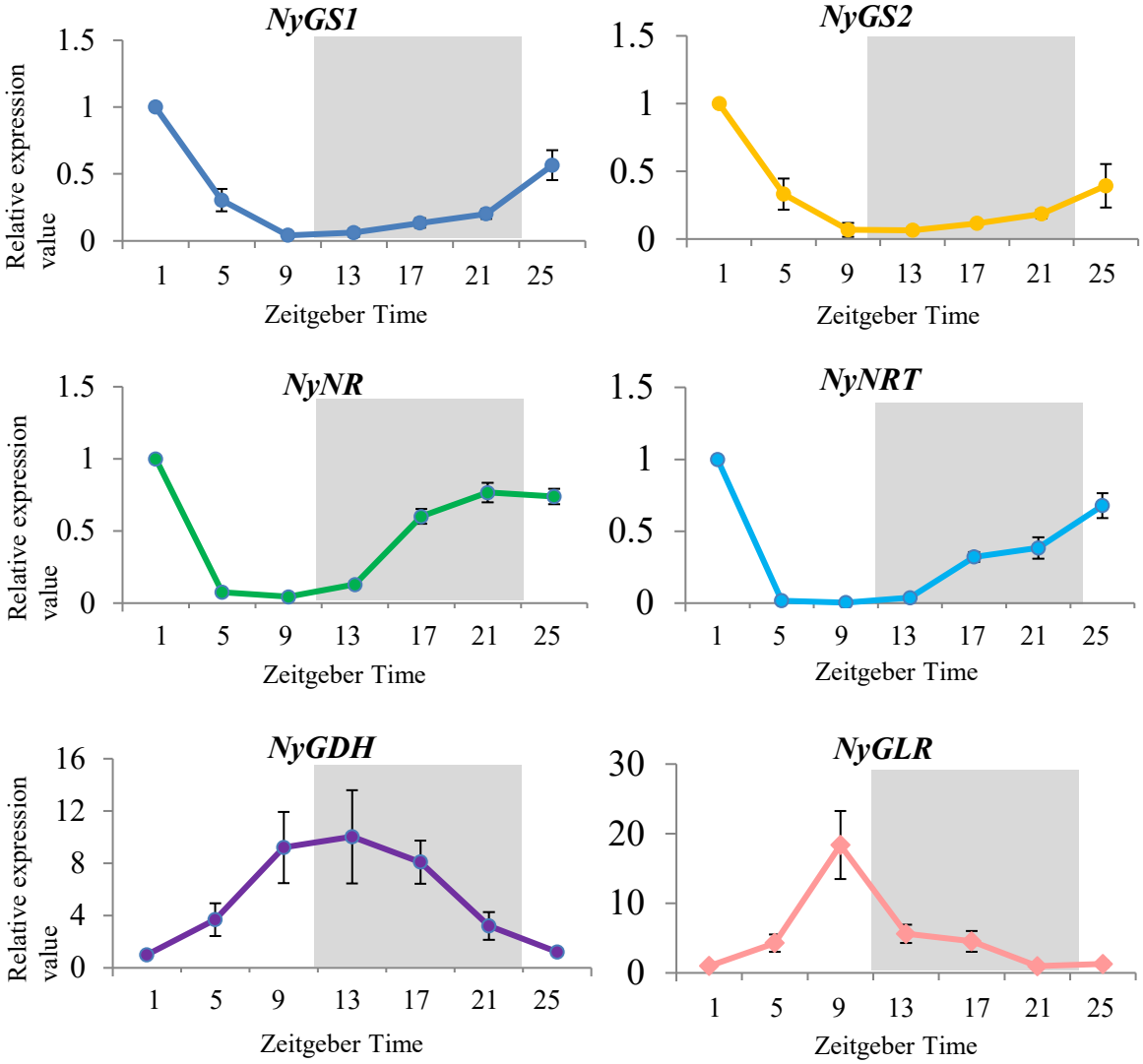
NyGS1
NyGS2
NyNR
NyNRT
NyGDH
NyGLR
Relative expression value
Zeitgeber Time
1 5 9 13 17 21 25

(B)

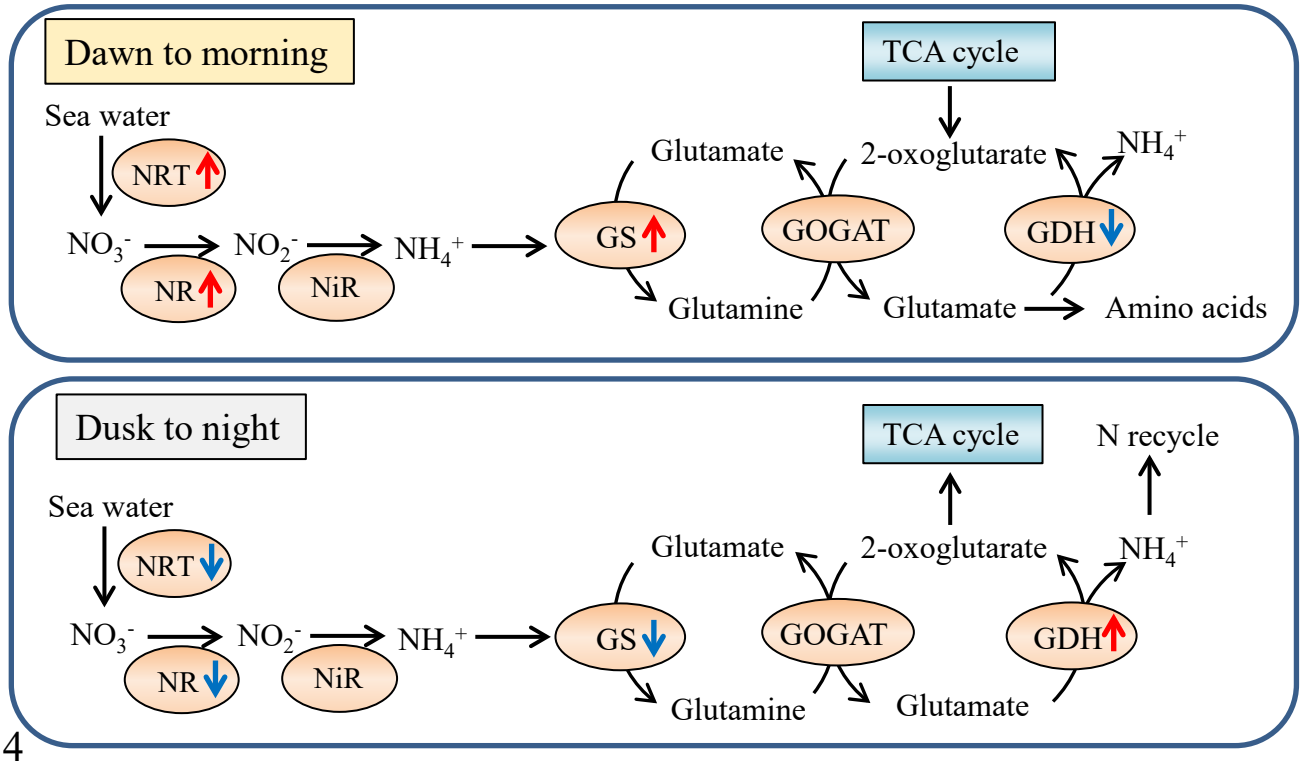
Dawn to morning
TCA cycle
Sea water
NRT
NO_3^-
NO_2^-
NH_4^+
NR
NiR
GS
Glutamate
2-oxoglutarate
GOGAT
GDH
Glutamine
Glutamate
Amino acids
Dusk to night
TCA cycle
N recycle
Sea water
NRT
NO_3^-
NO_2^-
NH_4^+
NR
NiR
GS
Glutamate
2-oxoglutarate
GOGAT
GDH
Glutamine
Glutamate

Fig. 4

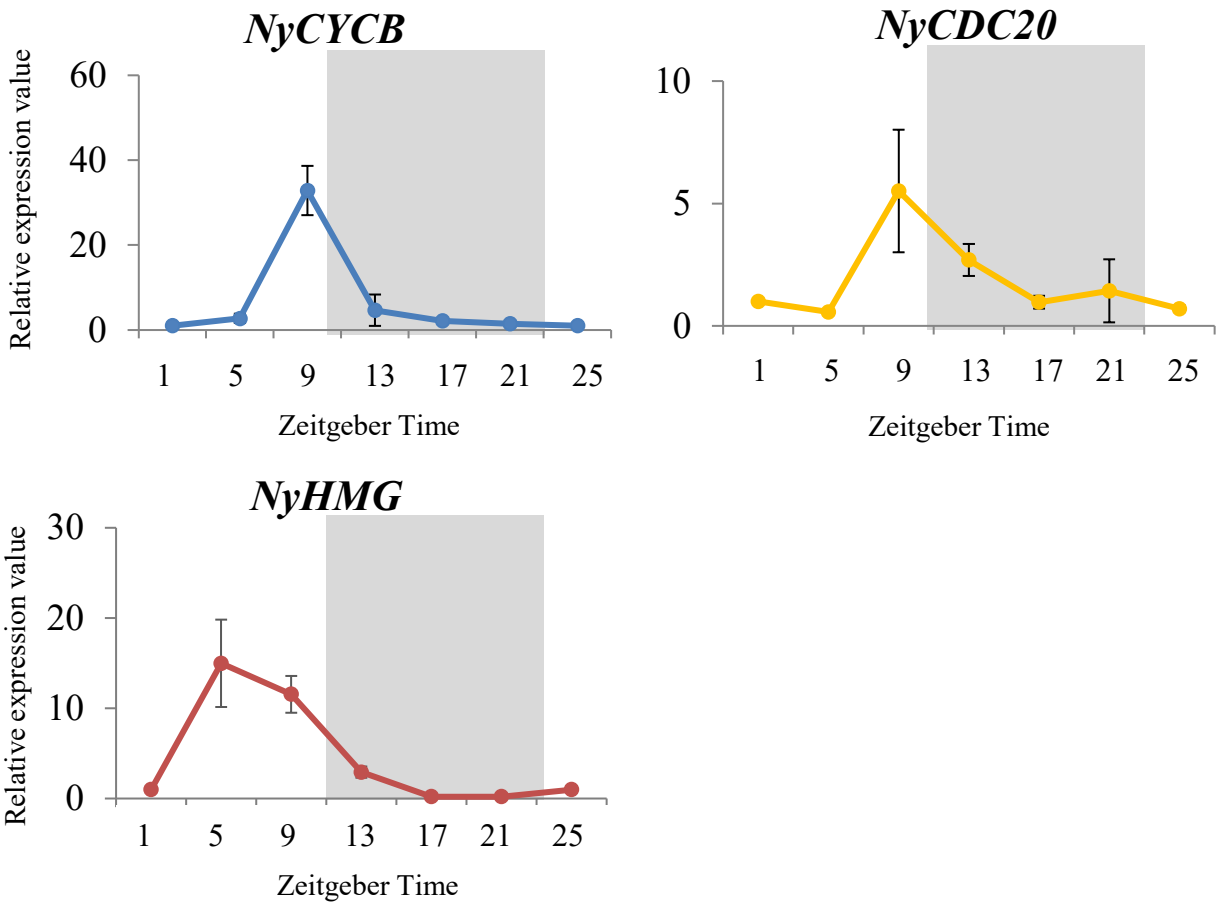
NyCYCB
Relative expression value
60
40
20
0
1
5
9
13
17
21
25
Zeitgeber Time
NyCDC20
10
5
0
1
5
9
13
17
21
25
Zeitgeber Time
NyHMG
Relative expression value
30
20
10
0
1
5
9
13
17
21
25
Zeitgeber Time

Fig. 5

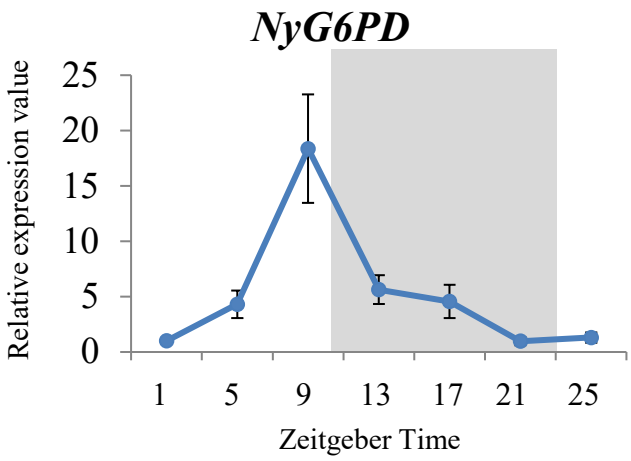
NyG6PD
Relative expression value
25
20
15
10
5
0
1
5
9
13
17
21
25
Zeitgeber Time

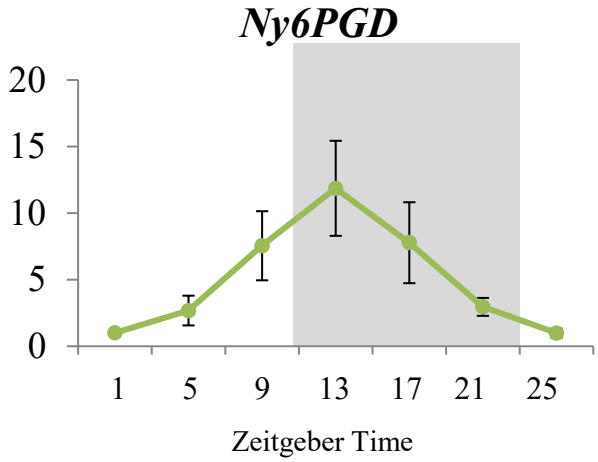
Ny6PGD
20
15
10
5
0
1
5
9
13
17
21
25
Zeitgeber Time

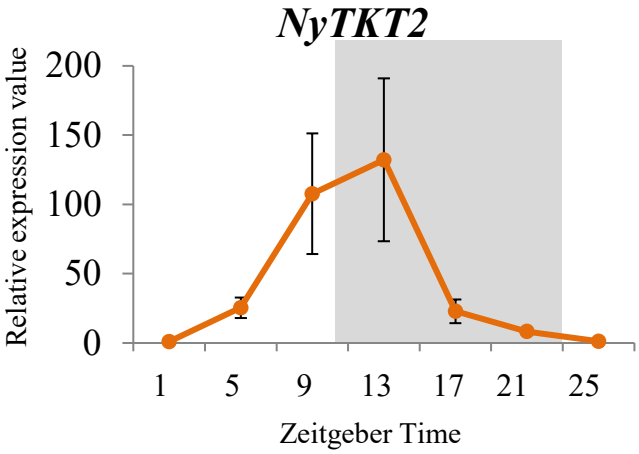
NyTKT2
Relative expression value
200
150
100
50
0
1
5
9
13
17
21
25
Zeitgeber Time

Fig. 6

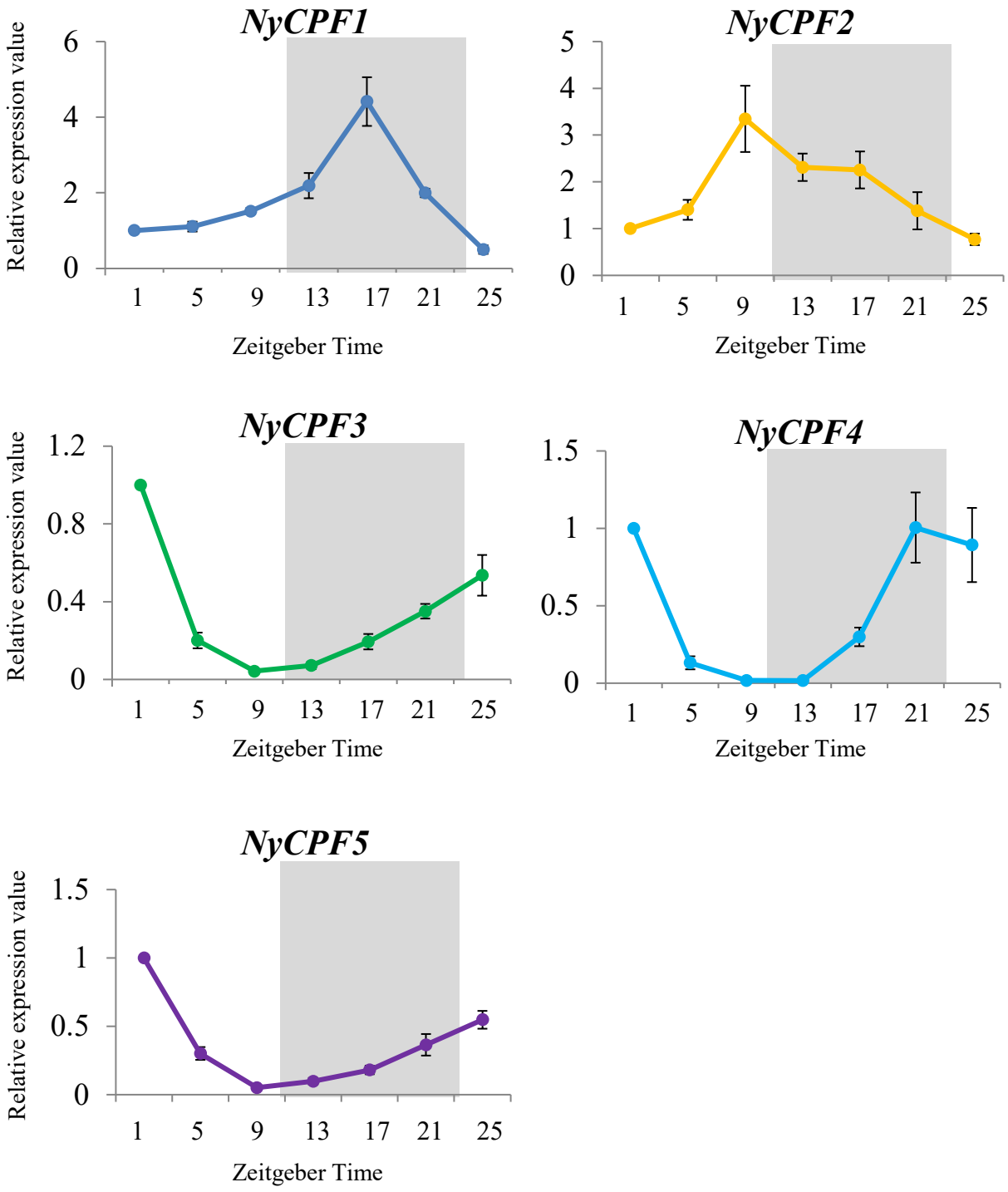
NyCPF1
Relative expression value
6
4
2
0
1
5
9
13
17
21
25
Zeitgeber Time
NyCPF2
5
4
3
2
1
0
1
5
9
13
17
21
25
Zeitgeber Time
NyCPF3
Relative expression value
1.2
0.8
0.4
0
1
5
9
13
17
21
25
Zeitgeber Time
NyCPF4
1.5
1
0.5
0
1
5
9
13
17
21
25
Zeitgeber Time
NyCPF5
Relative expression value
1.5
1
0.5
0
1
5
9
13
17
21
25
Zeitgeber Time

Fig. 7

Table 1. Summary of transcriptome analysis in *N. yezoensis* under light/dark cycles

Sample name	Raw reads	Clean reads Q30 (%)	Total mapped reads	Total mapping rate (%)
ZT1-1	25,040,424	91.42	13,103,477	57.24
ZT1-2	24,224,410	91.17	14,347,974	59.24
ZT9-1	22,613,710	91.23	11,370,577	55.11
ZT9-2	26,567,682	90.67	11,543,961	52.56

Table 2. The list of preferentially morning-phased genes in *N. yezoensis*

Contig ID	Abbreviation	Functional categories	Description	Fold Change ZT1 vs ZT9
contig_15570_g3725	PGK	carbohydrate biosynthesis	phosphoglyceratekinase	5.95
contig_8807_g2079	GAPDH	carbohydrate biosynthesis	glyceraldehyde-3-phosphate dehydrogenase	2.94
contig_18981_g4680	TPI	carbohydrate biosynthesis	triosephosphate isomerase	2.81
contig_11939_g2840	FBA	carbohydrate biosynthesis	fructose-1,6-bisphosphate aldolase	3.59
contig_12453_g2976	FBP	carbohydrate biosynthesis	fructose-1,6-bisphosphatase	2.62
contig_16120_g3879	TKT1	carbohydrate biosynthesis	transketolase 1	4.09
contig_7593_g1779	SBP	carbohydrate biosynthesis	sedoheptulose-1,7-bisphosphatase	2.79
contig_1528_g232	RPE	carbohydrate biosynthesis	ribulose-5-phosphate3-epimerase	5.17
contig_16198_g3910	RPI	carbohydrate biosynthesis	ribose-5-phosphate isomerase	2.52
contig_29611_g7274	PRK	carbohydrate biosynthesis	phosphoribulokinase	5.96
contig_25058_g6181	SIG	plastid transcription	sigma factor	3.67
contig_47994_g10351	HSP70	chaperone	heat shock protein 70	2.02
contig_4809_g1042	PPI	chaperone	peptidyl-prolyl cis-trans isomerase	3.83
contig_27230_g6699	Δ12Des	PUFA synthesis	delta-12 desaturase	4.92
contig_19105_g4720	Δ15Des	PUFA synthesis	delta-15 desaturase	4.37
contig_4519_g973	Δ5Des	PUFA synthesis	delta-5 desaturase	3.70
contig_14865_g3573	Δ6Des	PUFA synthesis	delta-6 desaturase	3.37
contig_19105_g4720	FAE	PUFA synthesis	fatty acid elongation enzyme	4.37
contig_8777_g2070	Δ9Des	PUFA synthesis	delta-9 desaturase	6.57
contig_11637_g2772	GS1	nitrogen metabolism	glutamine synthetase	2.93
contig_26825_g6597	GS2	nitrogen metabolism	glutamine synthetase	3.03
contig_15784_g3774	NRT	nitrogen metabolism	nitrate transporter	4.11
contig_14599_g3505	NR	nitrogen metabolism	nitrate reductase	3.75
contig_1166_g159	NiR	nitrogen metabolism	nitrite reductase	2.03
contig_22184_g5484	SBE	starch metabolism	starch branching enzyme	4.14
contig_17661_g4327	SS	starch metabolism	starch synthase	2.32
contig_25732_g6344	UGP	starch metabolism	UDP-glucose pyrophosphorylase	5.15
contig_22678_g5600	GK	proline metabolism	glutamate 5-kinase	3.28
contig_33403_g8066	FAL	extracellular matrix	fasciclin domain-containing protein	2.82
contig_2926_g600	CPF1	DNA repair/photoreceptor	cryptochrome-DASH 1	2.30
contig_4925_g1074	CPF2	DNA repair/photoreceptor	cryptochrome-DASH 2	2.49

Table 3. The list of preferentially evening-phased genes in *N. yezoensis*

Contig ID	Abbreviation	Functional categories	Description	Fold Change ZT1 vs ZT9
contig_7066_g1637	GDH	nitrogen metabolism	glutamate dehydrogenase	4.15
contig_21558_g5324	GLR	nitrogen metabolism	glutamate receptor-like	3.31
contig_6972_g1614	ASPG	asparagine metabolism	asparaginase	5.51
contig_43693_g9783	CYCB	cell cycle	cyclin B	5.06
contig_41863_g9511	3xHMG-box	cell division	3xHMG-box protein	3.28
contig_44008_g9836	CDC20	cell division	Cell division cycle protein 20	3.15
contig_30679_g7499	Pol ε	DNA synthesis/repair	DNA polymerase epsilon subunit	8.03
contig_13751_g3311	POLK	DNA synthesis/repair	DNA polymerase kappa	7.52
contig_31832_g7759	LIG4	DNA synthesis/repair	DNA ligase 4	7.72
contig_6499_g1481	PSF1	DNA synthesis/repair	DNA replication complex GINS protein PSF1	6.69
contig_16703_g4073	TOPII	DNA synthesis/repair	DNA topoisomerase II	3.14
contig_39232_g9109	RecQ	DNA synthesis/repair	RecQ family ATP-dependent DNA helicase	7.15
contig_30225_g7400	MCM2	DNA synthesis/repair	DNA replication licensing factor MCM2	2.53
contig_37946_g8902	SMC2	chromosome transmission	structural maintenance of chromosomes protein 2	7.21
contig_29724_g7290	SMC4	chromosome transmission	structural maintenance of chromosomes protein 4	2.59
contig_9037_g2150	6PGD	pentose phosphate pathway	6-phosphogluconate dehydrogenase	4.04
contig_28711_g7063	G6PD	pentose phosphate pathway	glucose-6-phosphate 1-dehydrogenase	3.54
contig_30474_g7461	TKT2	pentose phosphate pathway	transketolase 2	8.50
contig_33564_g8106	SPL4	extracellular matrix	spondin domain-containing protein 4	2.27
contig_3877_g849	MSIL	histone modification	MSI1-like WD40 repeat	2.87
contig_46867_g10259	SET	histone modification	SET-domain proteins	1.83
contig_24787_g6120	CPF3	DNA repair/photoreceptor	Cryptochrome/Photolyase family	2.75
contig_11984_g2852	CPF4	DNA repair/photoreceptor	Cryptochrome/Photolyase family	8.57
contig_24862_g6141	CPF5	DNA repair/photoreceptor	Cryptochrome/Photolyase family	2.55

Table S1. The list of primers used for gene expression analysis in *N. yezoensis*

Primer name	contig number	Sequence
Ny18SrRNA-F1	D79976[a]	AGGGTTGATCCGCAGGGAAG
Ny18SrRNA-R1		GCTTGCGCCCACTCCATTAG
NyNR-F1	contig_14599_g3505	ACGGAGGAGGACTCTTGGAT
NyNR-R1		GGCCAGCTCACCAATGTAAT
NyNRT-F1	contig_15784_g3774	TTTTCTCGTCGTTTGTGCAG
NyNRT-R1		ACCACAAAGCCCAGGTACAG
NyGS1-F1	contig_11637_g2772	CTGCCACACCAACTTCTCAA
NyGS1-R1		CCCCACGAGAACTTGTCAAT
NyGS2-F1	contig_26825_g6597	CCATCTACCCTGACCCCTTC
NyGS2-R1		GTCGAGATCAAGGAGCGTGT
NyGDH-F1	contig_7066_g1637	GCTTTGGTTGACAACGGAGT
NyGDH-R1		CTCCACCTTCTCAGCAGACC
NyGLR-F1	contig_21558_g5324	GCAGGAGCTGTTCTTTACGG
NyGLR-R1		TCAAACTGAGTGCCTTCACG
NyPGK-F1	contig_15570_g3725	CATCCTGCACCTTCCTCAGT
NyPGK-F1		AGACACAAATGCCATGGTGA
NyPRK-F1	contig_29611_g7274	GTCATTTGCCTGGACGACTT
NyPRK-R1		CCCGTCTCGTGGTTGTAGAT
NyCPF1-F1	contig_2926_g600	GACGTACGAGGAGCAGGAAG
NyCPF1-R1		AGACTCGCGGTAAGCAGTGT
NyCPF2-F1	contig_4925_g1074	TGGCTACCTTTCCAATCGAC
NyCPF2-R1		CAATGTACGCCCAGTTTTCC
NyCPF3-F1	contig_24862_g6141	CTCATCCCCCACTTTAAGCA
NyCPF3-R1		CAGCGTGTACTTGACGAGGA
NyCPF4-F1	contig_11984_g2852	GACATTGAGGTGAGCAACGA
NyCPF4-R1		GCATAAAGGACGCAAACTCC
NyCPF5-F1	contig_24787_g6120	CCCGATTTCCACTCGTACAT
NyCPF5-R1		GGAAACACCTCGTGGAGAAA
NyCYCB-F1	contig_43693_g9783	AATGGAGCGGTACATTCTGC
NyCYCB-R1		CAGACTGAGTTCCGACAGCA
NyCDC20-F1	contig_44008_g9836	CCTGAGATGCTCGACGACTA
NyCDC20-R1		ACGACACGGACGTCACATAG
NyHMG-F1	contig_41863_g9511	GTCGGCCTACCTCATCTTTG
NyHMG-R1		TCCATTTCCTTTTCGTACCG
Ny6PGD-F1	contig_9037_g2150	AAGGGCAGTCTCGACTCGTA
Ny6PGD-R1		AAAGACGGCCTCAGAGATGA
NyG6PD-F1	contig_28711_g7063	CCGGCTACTTCGACAACATT
NyG6PD-R1		GGTACACCCTCGTCGTCTGT
NyTKT1-F1	contig_16120_g3879	TGCGTACAAGCAGAGTGTCC
NyTKT1-R1		TTGAACAGCTCCATGACTGC
NyTKT2-F1	contig_30474_g7461	ATCTGGCCATGTCAGAGGAC
NyTKT2-R1		AACCCAATCGTCGTCACAAT
NyrbcL-F1	3978792[b]	GGTCCTGCAACTGGATTGAT
NyrbcL-R1		AGGAAATCAAGACCGCCTTT

[a]Accession number in GenBank, [b]Gene ID number

Table S2. The list of tested genes for validation of RNA-seq data

Contig ID	Abbreviation	Description
contig_11637_g2772	GS1	Glutamine synthetase
contig_7066_g1637	GDH	Glutamate dehydrogenase
contig_15784_g3774	NRT	Nitrate transporter
contig_14599_g3505	NR	Nitrate reductase
contig_9037_g2150	6PGD	6-phosphogluconate dehydrogenase
contig_15570_g3725	PGK	Phosphoglycerate kinase
contig_29611_g7274	PRK	Phosphoribulokinase
contig_44008_g9836	CDC20	Cell division cycle protein 20
contig_43693_g9783	CYCB	Cyclin B
contig_41863_g9511	HMG	3xHMG-box protein
contig_16120_g3879	TKT1	transketolase 1
contig_30474_g7461	TKT2	transketolase 2